Journal of Applied Polymer Science

Structural and Functional Changes of Silk Fibroin Scaffold Due to Hydrolytic Degradation

Mehdi Farokhi,[1] Fatemeh Mottaghitalab,[2] Jamshid Hadjati,[1] Ramin Omidvar,[3] Mohammad Majidi,[4] Amir Amanzadeh,[4] Mahmoud Azami,[1] Seyed Mohammad Tavangar,[1] Mohammad Ali Shokrgozar,[4] Jafar Ai[1]

[1]Department of Tissue Engineering, School of Advanced Technologies in Medicine, Tehran University of Medical Sciences, 43, Tehran, Iran

[2]Department of Nanobiotechnology, Faculty of Biological Sciences, Tarbiat Modares University (TMU), 124, Tehran, Iran

[3]Biomedical Engineering Department, Amirkabir University of Technology (Tehran Polytechnic), 78, Tehran, Iran

[4]National Cell Bank of Iran, Pasteur Institute of Iran, 69, Tehran, Iran

Correspondence to: Dr. M. A. Shokrgozar (E-mail: mashokrgozar@pasteur.ac.ir) or Dr J. Ai (E-mail: jafar_ai@tums.ac.ir)

ABSTRACT: In this study, hydrolytic degradation of silk fibroin (SF) in Phosphate buffer saline (PBS) after 12 weeks incubation was investigated. Fourier transform infrared spectroscopy (FTIR), Raman spectroscopy and X-ray diffraction (XRD) patterns have confirmed the transition from crystalline β-sheet to random coil in treated SF. A decrease in adhesion force and surface Young's modulus were observed using atomic force microscopy (AFM). Structural changes were further confirmed using scanning electron microscopy (SEM). Biocompatibility and alkaline phosphatase production of osteoblast cells were decreased significantly in treated SF scaffold. Moreover, a significant decrease in mRNA level of collagen type I and osteopontin compared with fresh SF scaffold was observed. Finally, structural and biological characteristics of SF scaffold could alter in PBS. © 2013 Wiley Periodicals, Inc. J. Appl. Polym. Sci. **2014**, *131*, 39980.

KEYWORDS: degradation; biocompatibility; properties; characterization

Received 16 June 2013; accepted 18 September 2013
DOI: 10.1002/app.39980

INTRODUCTION

An ideal scaffold for bone tissue engineering serves multiple purposes such as appropriate biocompatibility, osteoconductivity, structural properties, and so on.[1] Suitable degradation rate is another important parameter of the scaffold which should be considered for tissue regeneration.[2] Slow degradation rate may lead to fibrosis and lack of host integration.[3] In contrast, rapid degradation may collapse the porosity of artificial substitutes and could hinder the mass transfer.[4] Therefore, the balance between tissue formation and scaffold degradation is crucial. Various natural and synthetic polymers have been considered for bone tissue scaffolding. Among synthetic polymers, polylactic acid (PLA), polyglycolic acid (PGA), and polylactic glycolic acid (PLGA) usually degrade through hydrolysis and therefore their waste products could be removed from the body by metabolic pathways.[5] On the other hand, natural polymers such as collagen, fibrinogen, hyaluronic acid, and etc. are often more sensitive to enzymatic degradations in comparison to synthetic polymers.[6] Among natural biomaterials, silk fibroin (SF) is widely studied in the field of tissue engineering regarding to its biocompatibility, cell adhesion, and proliferation properties, minimal inflammatory response and superior linear stiffness. SF is categorized as a FDA approved polymer and degrades slowly *in vivo*, and for this, it is defined by the United States Pharmacopeia (USP) as nondegradable biomaterial.[7,8] The rate of SF biodegradation relies on the bulk crystallinity, structure, morphology, mechanical properties, and implantation site environment. SF as a protein could also degrade through enzymatic reaction such as proteolytic activity.[9–11] In contrast, SF scaffolds only loss 4% of their mass within 7 weeks through hydrolytic degradation.[12] Based on our knowledge, the response of osteoblast cells to SF has been rarely investigated so far. Therefore, it is necessary to evaluate whether long-time incubation in phosphate buffer saline (PBS) could affect the structure and bioactivity of SF constructs. Thus, this study represents the conformational changes of SF scaffold after 12 weeks incubation in PBS by using scanning electron microscopy (SEM), X-ray diffraction (XRD), Fourier Transform Infrared spectra (FTIR), Raman spectroscopy, differential scanning calorimetry (DSC), atomic force microscopy (AFM), and degradation study *in vitro*. In addition, biocompatibility, alkaline phosphatase (ALP) activity and real-time PCR were also inspected in order to evaluate the osteoblast cells response to the scaffold.

EXPRIMENTAL

Materials

Materials used in this research were purchased from Sigma-Aldrich (USA) including sodium carbonate, lithium bromide (LiBr), 3500 Da cut off dialysis tube, Dulbecco Modified Eagle's Medium (DMEM), Ham's F-12 Medium, fetal bovine serum (FBS), phosphate buffered saline (PBS), ascorbic 2-phosphate, penicillin, streptomycin, ketamine/xylazine, collagenase type I, [3-(4,5-dimethylthiazol-2-yl)-2,5-diphenyl tetrazolium bromide] (MTT), and isopropanol. In addition, ALP's kit were purchased from Pars azmun, Iran, RNeasy plus Mini kit from Qiagen, Germany and cDNA synthesis kit from TAKARA, Japan.

SF Scaffold Fabrication

Purification of SF has performed prior to scaffold fabrication. For this purpose, Bombyx mori silk fibers were degummed in 0.02 Na_2Co_3 for 1 h to extract sericin before being dissolved in 9.3 LiBr solution at 60°C for 4 h. To purify SF, 3500 Da cut off dialysis tube was used for 3 days (13). Afterwards, aqueous SF solution was poured into 24-well culture plate and placed in freeze-drying vessel (OHRIST BETA 1-15, Germany) for 10 h to form porous SF scaffolds. Finally, the SF scaffolds were immersed in PBS at 37°C for 12 weeks in order to evaluate the rate of hydrolytic degradation. Thereafter, two groups are considered for physical and chemical analysis: fresh SF as a control and treated SF (incubated in PBS).

Scanning Electron Microscopy (SEM)

Field emission scanning electron microscopy (FESEM; Quanta 200F, FEI, Oregon, US) at an accelerating voltage 15 kV was performed in order to evaluate the morphological structure of the scaffolds. In addition, the morphology of rabbit osteoblast cells seeded on the scaffolds was also examined. The samples were sputter-coated (Cressington 208 HR) with gold before the tests.

X-ray Diffraction (XRD)

X-ray diffraction (XRD) curves were recorded with an X-ray diffractometer (Xpert MPD, PANalytical, Netherland)). The X-ray source was Cu Ka (40 kV, 40 mA). The samples were scanned from 5 to 60 ° (2θ) at a scanning rate of 0.066°/min.

FTIR Spectroscopy

Attenuated total reflectance (ATR) on a fourier transform infrared (FTIR; Germany) spectrophotometer was performed on samples in the range of 650 cm^{-1} to 4000 cm^{-1} with spectral resolution of 4 cm^{-1} to evaluate the structural changes of samples.

Raman Spectroscopy

Raman spectroscopy (Almega Thermo Nicolet Dispersive Raman Spectrometer; Germany) was implemented in the spectral range of 100 cm^{-1} to 4200 cm^{-1} with resolution of 4 cm^{-1} in order to assess the physical and chemical structure of samples.

Differential Scanning Calorimetry (DSC)

The thermal stability of samples was evaluated using differential scanning calorimetry (DSC; NETZSCH, 200F3, Germany) with N_2 gas flow and heating rate of 10°C/min from 0°C to 350°C.

Atomic Force Microscopy (AFM)

The microstructure elasticity and adhesion force of fresh and treated SF scaffolds were measured by AFM. The samples were glued to the coverslip using three 0.5 μL droplets of cyanoacrylate adhesive[14] and then placed on the AFM stage. A Nanowizard2 AFM (JPK Instruments AG, Germany) was used to carry out the experiments. For AFM force mode scanning, a silicon AFM tip (CSC17/noAl, MikroMash) with a nominal spring constant of 0.15 N/m was used. The cone-shaped sharp tip was indented 3 μm to reach an indentation force of 5 nN. The speed of approach phase was set 1 μm/s and after 3 s pause time, the tip was retracted with the same speed. Between each two sampling locations, the system was paused for 5 s. The total examined points for each sample was 512 locations.

In Vitro Degradation

For *in vitro* degradation test, the samples were incubated in PBS (pH = 7.4) at 37°C after vacuum drying. The percentage of weight loss of SF scaffolds after different intervals was calculated using the following formula:

$$L=(W_0-W_1)/W_0,$$

L represents weight loss, W_0 represents the initial weight of the sample (mg), and W_1 represents the final weight of the sample (mg).[15]

Isolation of Osteoblast Cells

Osteoblast cells were isolated from male New Zealand rabbits (weight: 2.5–3 kg). At first, the rabbits were anesthetized and then sacrificed with an overdose administration of ketamine/xylazine. Each femur was then removed, rinsed and suspended in PBS. The bone tissues were cut into small pieces and digested with collagenase Type I (2.5 mg/mL) for 4 h at 37°C. After that, the digested bone were seeded into 25-cm^2-cell culture flask containing DMEM/Ham's F-12 medium supplemented with 10 FBS, 50 µg/mL ascorbic 2-phosphate, 100 U/mL penicillin, and 100 µg/mL streptomycin at 37°C in 5% CO_2. All experiments were performed using cells between third and sixth passage.

Biocompatibility

3-(4,5-dimethylthiazol-2-yl)-2,5-diphenyl tetrazolium bromide (MTT) was used in order to evaluate cell's viability next to the samples. Briefly, 2×10^4 of rabbit osteoblast cells were seeded on the scaffolds within a 96-well plate and were incubated at 37°C with 5% CO_2 for 5, 10, and 20 days. Afterward, scaffolds were removed and MTT at a concentration of 0.2 mg/mL was added to each well and incubated at 37°C for 4 h. The formazan produced by living cells was solubilized with isopropanol for 15 min and the absorbance was read at 570 nm using ELISA reader (BioTek microplate reader, USA). It should be mentioned that tissue culture polystyrene (TPS) was considered as negative control group.

Alkaline Phosphatase Assay (ALP Assay)

All stages were identical to the stages mentioned in MTT assay. Briefly, 10 μL supernatant of rabbit osteoblast cells was added to 1000 μL of ALP's kit (Pars Azmun, Ian) according to the manufacturer's protocol at 37°C to evaluate the ALP production of osteoblast cells at each time intervals (5, 10, and 20 days), by

Table I. Primer Sequences for Real-Time PCR

Direction	Abbreviations	Sequence of primers
Forward	GAPDH	5′ CGTCTGCCCTATCAACTTTCG 3′
Reverse	GAPDH	5′ CGTTTCTCAGGCTCCCTCT 3′
Forward	Collagen I	5′ GCGGTGGTTACGACTTTGGTT 3′
Reverse	Collagen I	5′ AGTGAGGAGGGTCTCAATCTG 3′
Forward	Osteopontin	5′ GCAGAATCTCCTAACACCGCAG 3′
Reverse	Osteopontin	5′ GGTCATCGTCCTCATCCTCATC 3′
Forward	Osteonectin	5′ AAGCCCTGCCTGATGAGACA 3′
Reverse	Osteonectin	5′ CCACTACTTCCTCTTCGGTTTCC 3′
Forward	RUNX2	5′ GGAGTGGACGAGGCAAGAGT 3′
Reverse	RUNX2	5′ AGGCGGTCAGAGAACAAACTAGG 3′

GAPDH: Glyceraldehyde-3-phosohate dehydrogenase.

conversion of p-nitrophenylphosphate to p-nitrophenol. The absorbance was read at 405 nm.

Real-Time PCR

The effect of fresh and treated SF scaffolds on rabbit osteoblast cells behavior was further evaluated by real-time quantitative RT-PCR (Applied Biosystems, Foster City, CA) in order to measure the mRNA expression of collagen type I (COL I), osteopontin (OP), osteonectin (ON) and RUNX2 (Table I). At first, the samples with diameters of $5\times5\times2$ mm^3 were placed into 24-well plastic culture plates and then a total of 10^5 osteoblast cells were seeded on the surface of the scaffolds. After 10 days incubation time, the cells were detached from the samples and total RNA isolated using RNeasy plus Mini kit according to the manufacturer's protocol. The amount of RNA pellet was measured by spectrophotometer (nanodrop, Germany) at the wavelength of 260/280 nm. Subsequently, RNA was converted to cDNA according to the manufacturer's instruction. Each reaction was performed in a total volume of 20 μL containing 5 μL cDNA sample, 10 µL Power SYBER Green PCR Master Mix (Applied Biosystems, USA), and 50 nM of each primers in final concentration. PCR reaction conditions were 15 min at 95°C, and then 40 cycles at 95°C for 15 s, and 1 min at 60°C. All samples were performed in quadruple and the house keeping gene, glyceraldehyde-3-phosphate-dehydrogenase (GAPDH), was used as an indigenous control.

Statistical Analysis

All of the quantitative data were expressed as means ± standard deviation. Statistical comparisons were performed using One way ANOVA with SPSS 16.0 (SPSS, USA). P values of less than 0.05 were considered statistically significant.

RESULTS

Scanning Electron Microscopy

Scanning electron microscopy micrographs were obtained from fresh and treated SF scaffolds. It is clear that the structure of freeze-dried SF constructs were mostly changed after 12-week incubation in PBS (Figure 1). It is evidenced that the interconnection between pores is degraded and thus larger pores with unusual structure are formed as a function of exposure time.

X-ray Diffraction (XRD)

Figure 2 shows the XRD pattern of fresh and treated SF scaffold, respectively. The fresh SF scaffold has shown a sharp peak at $2\theta = 20^\circ$ which is attributed to crystalline β-sheet conformation [Figure 2(a)]. Conversely, degradation of SF scaffold after

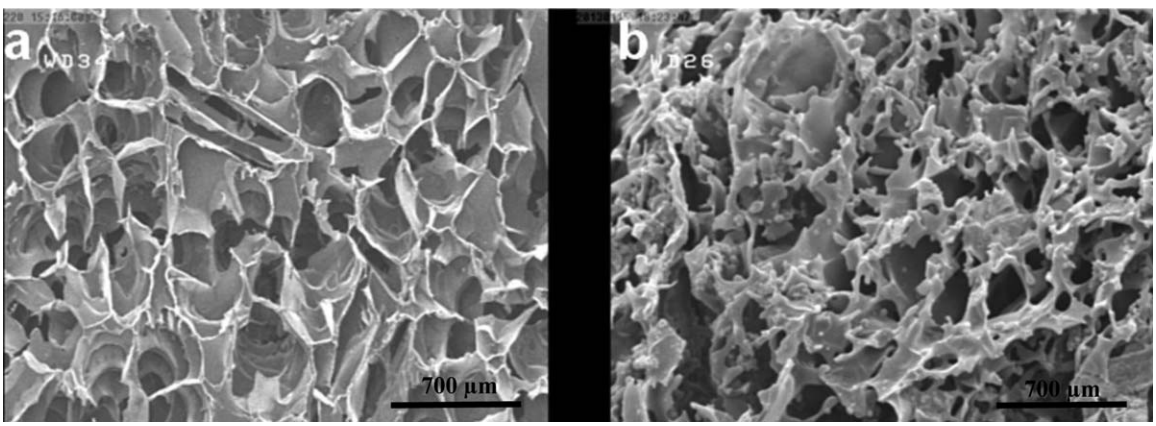

Figure 1. Scanning electron micrographs of: (a) Fresh SF scaffold, (b) Treated SF scaffold in PBS after 12 weeks. The interconnection between pores is treated and larger pores with unusual structure are formed as a function of exposure time.

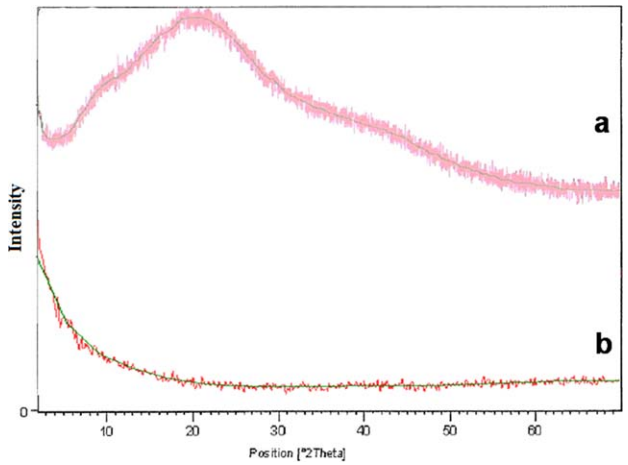

Figure 2. XRD pattern of: (a) Fresh SF scaffold with a sharp peak at $2\theta = 20^{\circ}$attributed to crystalline β-sheet conformation, (b) Treated SF scaffold: the peak at $2\theta = 20^{\circ}$ has disappeared which confirms the transition from β-sheet to random coil after 12 weeks degradation in PBS. [Color figure can be viewed in the online issue, which is available at wileyonlinelibrary.com.]

12 weeks lead to transition to random coil and thus the peak at $2\theta=20^{\circ}$ has disappeared [Figure 2(b)].

FTIR Spectroscopy

As shown in Figure 3(a), SF scaffold has typical peaks in 1227 cm^{-1} (amide III), 1527 cm^{-1} (amide II), and 1625 cm^{-1} (amide I) introducing β-sheet conformation. It is obvious that after treating SF scaffold in PBS for 12 weeks, these characteristic peaks did not shift in term of position [Figure 3(b)]. Moreover, an increase in intensity of peaks related to amide groups was observed.

Raman Spectroscopy

Figure 4 displays the Raman spectra of SF scaffold before and after incubation in PBS. A characteristic peaks corresponding to

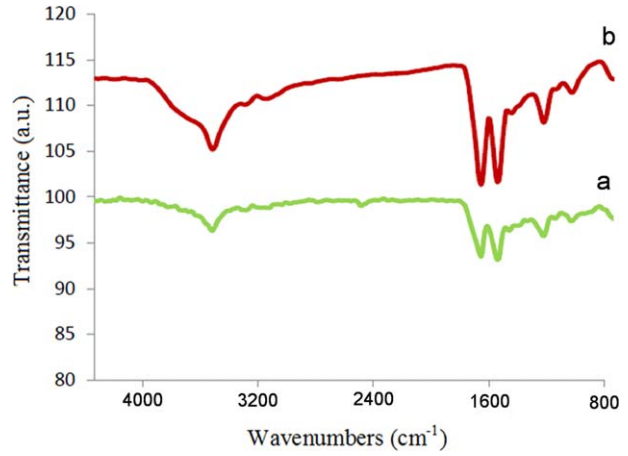

Figure 3. FTIR spectra of: (a) Fresh SF scaffold: the typical peaks in 1227 cm^{-1} (amide III), 1527 cm^{-1} (amide II), 1625 cm^{-1} (amide I) introduce β-sheet conformation. (b) Treated SF scaffold: the mentioned characteristic peaks were intensified due to weakening of peptide bond. [Color figure can be viewed in the online issue, which is available at wileyonlinelibrary.com.]

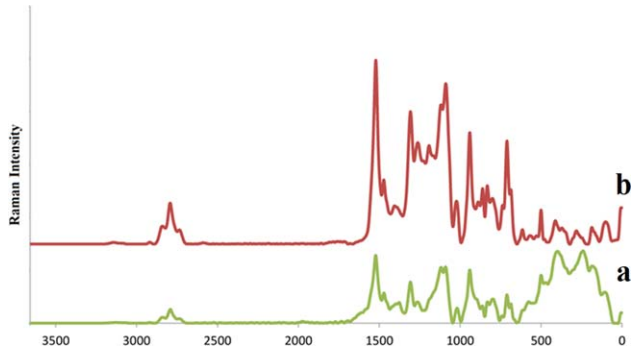

Figure 4. Raman signature of: (a) Fresh SF scaffold, (b) Treated SF scaffold. The peaks corresponding to fresh SF scaffold were intensified after incubation. It is suggested that PBS could interact with polar groups in the backbone of SF scaffold and thus interfere the hydrogen bindings. [Color figure can be viewed in the online issue, which is available at wileyonlinelibrary.com.]

fresh SF scaffold is intensified after incubation in PBS. It is suggested that PBS could interact with polar groups in the backbone of SF scaffold and thus interfere the hydrogen bindings. For this reason, nonpolar hydrophobic amino acids such as Ala, Leu, Ileu, and Val will be released and this could change the intensity of peak regarding to aliphatic C-C in the structure of SF scaffold.

Differential Scanning Calorimetry (DSC)

DSC data shows the spatial organization of SF scaffold before and after incubation in PBS (Figure 5). The pattern demonstrates an endothermic peak at about 283°C and 281°C attributed to thermal decomposition of fresh SF scaffold and treated SF scaffold, respectively. It is evidenced that thermal decomposition of SF at about 280°C is attributed to β-sheet conformation. Moreover, a second peak at 82.3°C regarding to the loss of water during heating was appeared for fresh SF scaffold while this temperature was decreased to 73°C for treated SF scaffold.

Atomic Force Microscopy (AFM)

Figure 6(a) shows the histogram and Gaussian fit for both Young's modulus and adhesion force between two samples. The

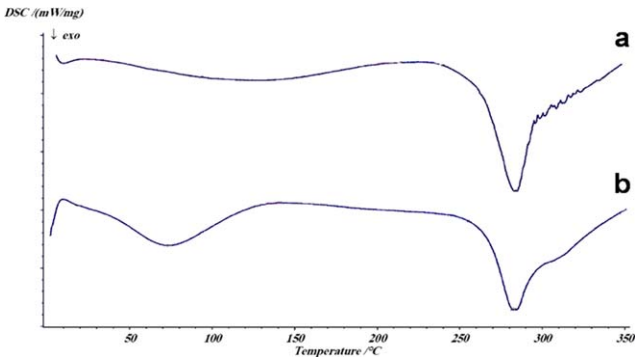

Figure 5. DSC curve of: (a) Fresh SF scaffold, (b) Treated SF scaffold. The pattern demonstrates an endothermic peak at about 283°C and 281°C attributed to thermal decomposition of fresh SF scaffold and treated SF scaffold, respectively. It is suggested that less changes are occurred in thermal stability of SF scaffold after incubation in PBS for 12 weeks. [Color figure can be viewed in the online issue, which is available at wileyonlinelibrary.com.]

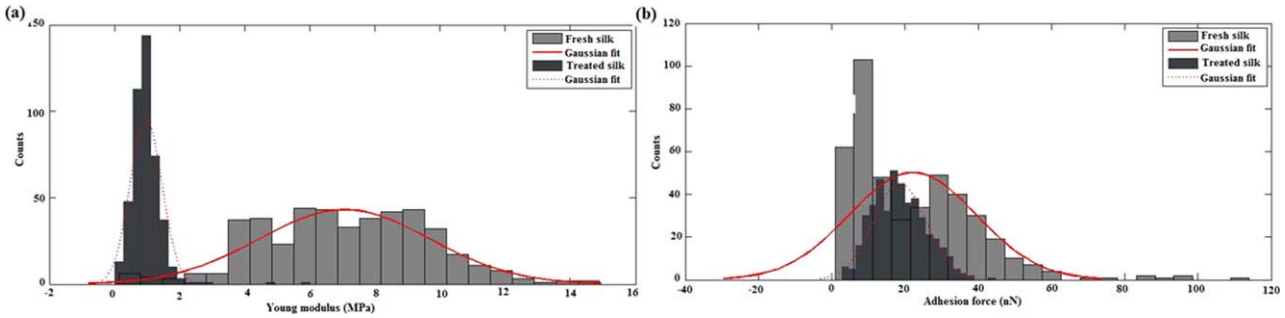

Figure 6. (a) Elasticity histogram and Gaussian fit for fresh SF scaffold as a control and treated SF scaffold. The average value for fresh SF scaffold was 7.06 ± 2.66 and for treated SF scaffold is 0.97 ± 0.49. (b) Adhesion force histogram and Gaussian fit for both materials. The difference between average values was not significantly wide however the control's data has greater deviations. The average value for fresh and treated silk was obtained18.58± 2.73 nN and 22.11 ± 17.24, respectively. [Color figure can be viewed in the online issue, which is available at wileyonlinelibrary.com.]

results have shown that the Young's modulus of treated SF scaffold have decreased than the control sample (fresh SF scaffold) significantly ($P < 0.05$). The average of elastic modulus for control and incubated SF scaffold was 0.97 ± 0.49 and 7.06 ± 2.66 MPa, respectively. Contrary to elasticity, the adhesion force between SF and cantilever did not show a notable variation after incubation [Figure 6(b)]. The Gaussian curves gave the average value for adhesion force about 18.58± 2.73 nN for incubated SF scaffold while the fresh SF scaffold had a value of 22.11±17.24 nN.

In Vitro Degradation of SF Scaffold

The *In vitro* degradation behaviors of SF scaffold in PBS solution were assessed at 37°C up to 12 weeks. Minimal solubilization and degradation in SF mass was observed after 12 weeks (Figure 7).

Biocompatibility

It is confirmed that the degradation rate of porous scaffold could affect the cells viability, attachment and host immune response. For this, the biocompatibility of treated SF scaffold was assessed. Surprisingly, the obtained result showed that the osteoblast cells viability decreased significantly ($P < 0.05$) in comparison to TPS and fresh SF scaffold after exposure time (Figure 8). However, the proliferation of cells on fresh SF scaffold was approximately similar to TPS.

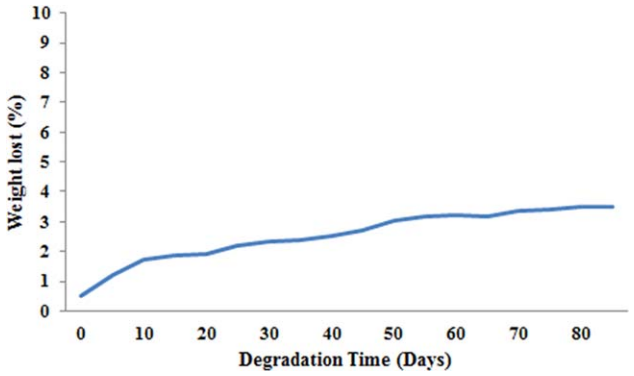

Figure 7. Degradation ratio of SF scaffold during degradation *in vitro*. [Color figure can be viewed in the online issue, which is available at wileyonlinelibrary.com.]

ALP Production Assay

ALP as a marker for differentiating osteoblasts could maintain osteoblastic phenotype during proliferation. The pattern of ALP production was similar to MTT assay (Figure 9). Treated SF scaffold exhibited lower ALP production in comparison to TPS and fresh SF scaffold at different time intervals (5, 10, and 20 days). Conversely, ALP production did not show any differences between TPS and fresh SF scaffold.

Expression of Osteoblast Genes

The mRNA expression of osteoblast cells on fresh and treated SF scaffolds were compared with TPS as a control group. It should be noticed that mRNA expression of cells in TPS group was taken as 100%. Generally, our results revealed that osteoblast cells expressed all bone gene markers in all groups after exposure time. The mRNA level of collagen type I (COL I) was significantly decreased in treated SF scaffold in comparison to fresh SF and TPS [Figure 10, ($P < 0.05$)]. Furthermore, the gene expression of Osteopontin (OP) was significantly downregulated in treated SF scaffolds compared to fresh SF scaffold and TPS groups ($P < 0.05$). Conversely, the mRNA expression

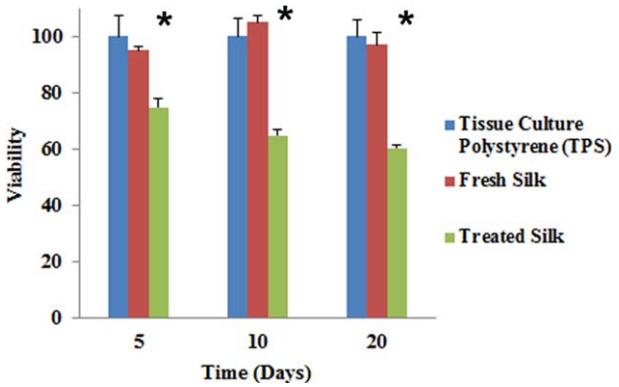

Figure 8. Viability of osteoblast cells on fresh and treated SF scaffolds were compared with TPS and fresh SF scaffold (*$P < 0.05$). The osteoblast cells viability of treated SF scaffold decreased significantly in compared with TPS and fresh SF scaffold after all times incubation. However, the proliferation of cells on fresh SF scaffold was approximately similar to TPS. [Color figure can be viewed in the online issue, which is available at wileyonlinelibrary.com.]

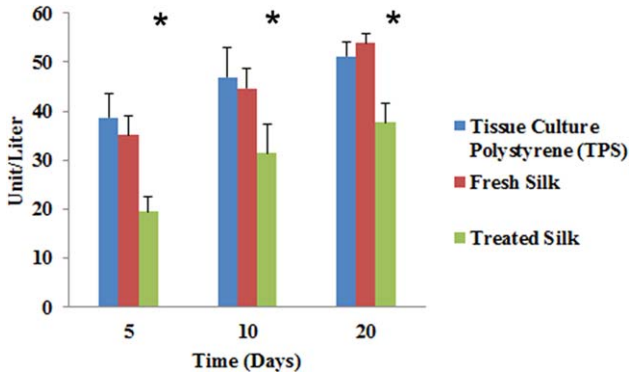

Figure 9. ALP activity of osteoblast cells next to fresh and treated SF scaffolds were compared with TPS and fresh SF scaffold (*$P < 0.05$). Treated SF scaffold surface exhibited lowest ALP production in comparison to TPS and untreated SF scaffold at various time intervals (5, 10, and 20 days). [Color figure can be viewed in the online issue, which is available at wileyonlinelibrary.com.]

pattern of osteonectin (ON) and RUNX2 were relatively stable (Figure 10).

DISCUSSION

The degradability of a scaffold should be amendable to kinetically match the evolving environment during tissue regeneration and healing. It is important to find the relationships between scaffold biodegradation rate and bone regeneration *in vitro* and *in vivo*. It has been demonstrated that slow degradation of collagen matrix in defected bone could enhance the process of osteogenesis.[16] Moreover, the integrity of load-bearing systems is related to degradability of polymers. However, fast degradation rate of many polymers might interfere the integrity of the system.[4,17] In this study, we have evaluated whether long-time incubation of SF in PBS could affect the structure and bioactivity of SF based scaffold. For this purpose, various analytical tools were performed in the present study to assess the features of SF based scaffolds prior and after incubation of SF in PBS. SEM images have shown that the walls between pores in the structure of porous SF scaffold were degraded and thus larger pores with unusual structure are formed on the surface of scaffold. Similarly with our observation, electrospun SF scaffolds incubated in PBS for 18 days and 24 days showed a few visible holes resulted from the surface erosion where the quantity of the holes slightly increased with increasing exposure time.[2,18] It is suggested that amorphous regions exists in the structure of SF lead to hole formation. To confirm the conformational changes of SF scaffold, X-ray diffraction were examined. Incubation of SF scaffold in PBS for 12 weeks leads to transition from crystalline β-sheet to random coil. This result is in agreement with those obtained by She et al. indicating that degradation of silk fibroin/chitosan after 6 weeks has changed the crystalline structure of silk from β-sheet to random coil.[15] Moreover, in contrast to our findings, Zhou et al. demonstrates that incubated silk in PBS have shown less conformational changes after 24 days while preserving it β-sheet structure. This may be attributed to short incubation time of silk scaffold in PBS in comparison to our study. Additionally, the result concerning FTIR spectra demonstrated an increase in intensity of amide characteristic peaks after incubation in PBS related to the transition of β-sheet to random coil (Figure 3). This change may be due to the weakening of the peptide bond in the structure of SF scaffold. Some studies have reported that the increase in the intensity of amide bonds indicates the transition of β-sheet to random coil.[19,20] In addition, it was shown by others that incubating silk in PBS could change its structural conformation during long periods and thus lead to transition from β-sheet to random coil.[2] In contrast with our observations, Horan et al. have shown that the structure of silk was essentially unchanged during 70 days with perhaps some slight loss of crystalline (β-sheet) material either directly due to hydrolysis or due to loss of crystalline material into the solution as the non-crystalline domains are digested.[11] It is appeared that the type of processing method for fabrication of SF constructs might affect the structural behavior of SF scaffold after incubation in PBS. Horan et al. have fabricated SF matrix containing wire-rope like fibers while in our study the SF scaffold was fabricated using freeze-drying. It is suggested that penetration of PBS into the porous structure of freeze-dried SF and subsequent hydrolysis is more than SF matrix with wire-rope like fibers. Therefore, the structural changes of porous scaffold are more obvious than those described previously.

To further analyze the structural changes of SF-based scaffold at molecular level, Raman spectroscopy was performed. The results have shown that the characteristic peaks of SF could be changed due to the interaction between PBS and polar groups in the backbone of SF.[18] In consistence with our study, She et al. have stated that hydrophilic agents such as PBS could cleavage the hydrolytically sensitive peptide bonds and glycoside bonds during degradation process.[13] In our study, for instance a peak at 1262 cm^{-1} is enhanced in treated SF which is correspondent to amide III in α-helix and random coil conformations (Figure 4). It is recommended that due to incubation of SF in PBS for 12

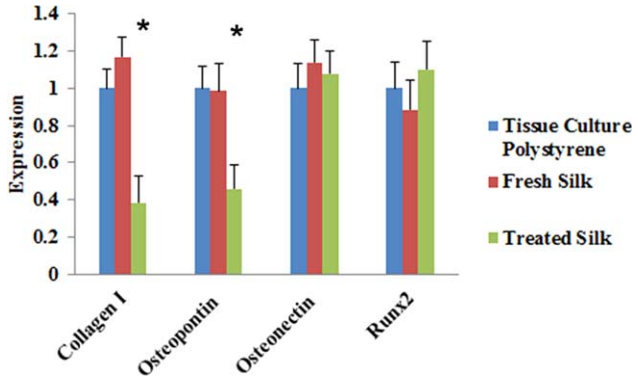

Figure 10. Genes expression of osteoblast cells on fresh and treated SF scaffolds in comparison to TPS as a control group. mRNA levels of collagen I was significantly decreased in treated SF scaffold in comparison to fresh SF scaffold and TPS. Gene expression of osteopontin was significantly down-regulated in treated SF scaffolds compared with fresh SF scaffold and TPS groups ($P < 0.05$). The mRNA expression pattern of osteonectin and RUNX2 were relatively stable and did not show any difference between all mentioned groups. [Color figure can be viewed in the online issue, which is available at wileyonlinelibrary.com.]

weeks, the β-sheet conformation has changed.[21] It has been proven that the mechanical properties of the environment are one of the effective elements which cause different signaling pathways and consequently different behaviors. Besides, it has been observed that different mechanical properties of matrices induce differentiation of stem cells to different target cells.[22] In the current work, AFM results have confirmed that the incubation of SF scaffold in PBS could decrease the Young's modulus, significantly. This could be attributed to surface degradation of silk fibroin and this demonstrate that hydrolytic degradation of porous SF scaffolds in PBS could affect the surface mechanical properties. In contrast, the adhesion force has not changed. Similarly, the results concerning DSC analysis have demonstrates that fewer changes are occurred in thermal stability of SF after incubation in PBS for 12 weeks. Minimal solubilization and degradation in SF mass was also observed after 12 weeks. This finding is compatible with previous studies indicating that incubation of silk based materials in buffer without enzyme has not changed the mass significantly.[23,24] However, Li et al. has shown that the weights of silk fibroin sheet in PBS rapidly decreased to ~70% of the pretreatment weights and reach 68% after 15 days.[18] Li et al has stated that incubation of silk in PBS could release the non-crosslinked proteins with low molecular weight and this could result in the mass loss of silk fibroin. Previous works implied that the rate of degradation may affect cellular interaction including cell proliferation, tissue regeneration and host response.[25,26] In this work, the response of osteoblast cells on the scaffold was also assessed. Concurrently, the biocompatibility and ALP production were decreased in treated SF scaffold, significantly. It was reported that that biodegradation of SF could produce nontoxic materials which have not harmful effect on cellular behavior *in vitro* and *in vivo*.[27] However, this discrepancy with our observation could be resulted from SF surface chemical and structural changes after 12-week incubation. A reason for this observation is the change in porous structure of the SF scaffold after incubation time as confirmed by SEM. This might induce low infiltration and subsequently proliferation of cells within the SF matrix. The architecture, mechanical and biochemical properties of a matrix could affect the interaction between cells and environment. Therefore, scaffolds with different structural and mechanical properties have diverse effect on cellular behavior and function.[28] Stiffness of the scaffold causes machanotransductive responses by cells mediated by biochemical cues such as cytoskeleton.[29] Some studies reported that stiff scaffolds could enhance cells proliferation and differentiation than compliant scaffold. According to our result, the stiffness of treated scaffold was decreased significantly. This issue may consider as an additional reason that decreased osteoblast cells proliferation on the fabricated scaffold.[30,31]

In consistent with MTT results, ALP production was also decreased as respected. It is confirmed that ALP activity is sensitive to osteoblast cells density as suggested by other workers.[33,34] Thus, the low proliferation and infiltration of cells within the scaffold could also be involved in the decrease in ALP production. Park et al. reported that ALP production of human bone marrow stem cell next to aqueous derived silk scaffold significantly decreased after 56 days incubation compared with Day 16.[35] It should be concluded that long time incubation of SF in aqueous environment could affect the proliferation of osteoblast cells and subsequently ALP production. The gene expression pattern is another important parameter to find cells response to different environment. The expression of COL I which implies the proliferation activity of bone cells[36–38] was decreased in treated SF based scaffold. The changes of treated SF scaffold suggests that the decrease in cellular proliferation and COL I expression, subsequently. Similarly, the gene expression of OP, as a matrix mineralization protein, was significantly down-regulated in treated SF scaffolds compared with fresh SF and TPS groups. OP is responsible for cell attachment at bone remodeling sites.[39,40] It should be emphasized that scaffold's characteristics such as surface topography, chemistry (wettability, softness and stiffness, roughness); microstructure (porosity, pore size, pore shape, interconnectivity, specific surface area)[41] and mechanical properties[42,43] have been shown to significantly affect the cellular performances for example adhesion, growth, differentiation and the bioactivity of scaffolds *in vitro* and *in vivo*. It is suggested that treated SF scaffold could not provide an appropriate surface for cellular attachment due to change in surface topography, microstructure and mechanical properties and thus the mRNA level of COL I and OP has decreased. Conversely, the mRNA expression pattern of ON as a structural protein of bone tissue[44] and RUNX2 as a transcription factor for controlling osteoblastic differentiation and maturation,[45] were relatively stable. Taken together, these results suggest that the treated SF scaffold did not affect the osteogenic differentiation and maturation but could alter the osteoblastic proliferation and attachment. Totally, the results indicated that incubating SF in PBS could change the structural, physical, mechanical properties of the scaffold.

CONCLUSIONS

Biodegradability is an important parameter for fabricating scaffolds in tissue engineering applications. In this study, a freeze-dried SF scaffold was immersed in PBS solution for 12 weeks at 37°C in order to evaluate its biodegradation properties *in vitro*. The results indicate that incubating SF in PBS could change the structural, physical, mechanical properties of the scaffold. Subsequently, the behavior of osteoblast cells may alter in terms of biocompatibility, ALP production and even some bone gene markers expression. These findings confirm the structural characteristics of SF scaffold as a result of hydrolytic degradation in PBS.

ACKNOWLEDGMENTS

The authors thank to the staffs of Tehran University of Medical Science and National Cell Bank of Pasteur Institute of Iran for their cooperation and useful consultation.

REFERENCES

1. Habibovic, P.; Yuan, H.; Van den Doel, M.; Sees, T. M.; Van Blitterswijk, C. A.; De Groot, K. *J. Orthop. Res.* **2006**, *24*, 867.
2. Zhou, J.; Cao, C.; M., X.; Hu, L.; Chen, L.; Wang, C. *Polym. Degrad. Stab.* **2010**, *95*, 1679.
3. Sanz-Herrera, J. A.; Garcia-Aznar, J. M.; Doblare, M. *Acta Biomater.* **2009**, *5*, 219.

4. Drury, J. L.; Mooney, D. J. *Biomaterials* **2003**, *24*, 4337.
5. Athanasiou, K. A.; Shah, A. R.; Hernandez, R. J.; LeBaron, R. G. *Clin. Sports Med.* **2001**, *20*, 223.
6. Dawson, E.; Mapili, G.; Erickson, K.; Taqvi, S.; Roy, K. *Adv. Drug Deliv. Rev.* **2008**, *60*, 215.
7. Altman, G. H.; Diaz, F.; Jakuba, C.; Calabro, T.; Horan, R. L.; Chen, J.; Kaplan, D. L. *Biomaterials* **2003**, *24*, 401.
8. Vunjak-Novakovic, G.; Altman, G.; Horan, R.; Kaplan, D. L. *Annu. Rev. Biomed. Eng.* **2004**, *6*, 131.
9. Wenk, E.; Merkle, H. P.; Meinel, L. *J. Controlled Release* **2011**, *150*, 128.
10. Arai, T.; Freddi, G.; Innocenti, R.; Tsukada, M. *J. Appl. Polym. Sci.* **2004**, *91*, 2383.
11. Horan, R. L.; Antle, K.; Collette, A. L.; Wang, Y.; Huang, J.; Moreau, J. E.; Altman, G. H. *Biomaterials* **2005**, *26*, 3385.
12. Wenk, E.; Meinel, A. J.; Wildy, S.; Merkle, H. P.; Meinel, L. *Biomaterials* **2009**, *30*, 2571.
13. Wang, Y.; Bella, E. S. D.; Lee, C.; Migliaresi, C.; Pelcastre, L.; Schwartz, Z.; Boyan, B.; Motta, A. *Biomaterials* **2010**, *31*, 4672.
14. Stefania Puttini, M. L. *Mol. Therapy* **2008**, *17*, 19.
15. She, Z.; Zhang, B.; Jin, C.; Feng, Q.; Xu, Y. *Polym. Degrad. Stab.* **2008**, *93*, 1316.
16. Andermahr, J.; Elsner, A.; Brings, A. E.; Hensler, T.; Gerbershagen, H.; Jubel, A. *J. Neurotrauma* **2006**, *23*, 708.
17. Pachence, J. M.; Bohrer, M. P.; K. J. In Lanza, R.; Langer, R.; Vacanti, J., Eds. Academic Press, 2007, 323–339.
18. Li, M.; Ogiso, M.; Minour, N. *Biomaterials* **2003**, *24*, 357.
19. Kojthung, A.; Meesilpa, P.; Sudatis, B.; Treeratanapiboon, L.; Udomsangpetch, R.; Oonkhanond, B. *Int. Biodeter. Biodegr.* **2008**, *62*, 487.
20. Tsuboi, Y.; Ikejiri, T.; Shiga, S.; Yamada, K.; Itaya, *Appl. Phys. A Mater. Sci. Process.* **2001**, *73*, 637.
21. Monti, P.; Taddei, P.; Freddi, G.; Asakura, T.; Tsukada, M. *J. Raman Spectrosc.* **2001**, *32*, 103.
22. Engler, A. J.; Sen, S.; Sweeney, H. L.; Discher, D. E. *Cell* **2006**, *126*, 677.
23. Wittmer, C. R.; Hu, X.; Gauthier, P. C.; Weisman, S.; Kaplan, D. L.; Sutherland, T. D. *Acta Biomater.* **2001**, *7*, 3789.
24. Yang, Y.; Zhao, Y.; Gu, Y.; Yan, X.; Liu, J.; Ding, F.; Gu, X. *Polym. Degrad. Stab.* **2009**, *94*, 2213.
25. Babensee, J. E.; Anderson, J. M.; Mclntire, L. V.; Mikos, A. G. *Adv. Drug Deliver. Rev.* **1998**, *33*, 111.
26. Lewandrowski, K. U.; Grosser, J. D.; Wise, D. L.; Trantolo, D. J.; Hasirci, V. *J. Biomater. Sci. Polym. Ed.* **2000**, *11*, 401.
27. Wenk, Merkle, H. P.; Meinel, L. *J. Controlled Release* **2011**, *150*, 128.
28. Dado, D.; Levenberg, S. *Seminars Cell Dev. Biol.* **2009**, *20*, 656.
29. Ingber, D. E. *FASEB J.* **2006**, *20*, 811.
30. Hadjipanayi, E.; Mudera, V.; Brown, R. A. *J. Tissue Eng. Regen. Med.* **2009**, *3*, 77.
31. Levenberg, S.; Huang, N. F.; Lavik, E.; Rogers, A. B.; Itskovitz-Eldor, J.; Langer, R. *Proc. Natl. Acad. Sci. USA* **2003**, *100*, 12741.
32. Ghosh, K.; Pan, Z.; Guan, E.; Ge, S.; Liu, Y.; Nakamura, T.; Clark, R. A. *Biomaterials* **2007**, *28*, 671.
33. Beresford, J. N.; Gallagher, J. A.; Russell, R. G. *Endocrinology* **1986**, *119*, 1776.
34. Stein, G. S.; Lian, J. B. *Endocr. Rev.* **1993**, *14*, 424.
35. Park, S. H.; Gil, E. S.; Shi, H.; Joo Kim, H.; Lee, K.; Kaplan, D. L. *Biomaterials* **2010**, *31*, 6162.
36. Glimcher, M. J. *Anat. Rec.* **1989**, *224*, 139.
37. Glimcher, M. J. *Biomaterials* **1990**, *11*, 7.
38. Mundlos, S. *Prog, Histochem, Cytochem,* **1994**, *28*, 1.
39. Kasugai, S.; Nagata, T.; Sodek, J. *J. Cell Physiol.* **1992**, *152*, 467.
40. Alford, A. I.; Hankenson, K. D. *Bone* **2006**, *38*, 749.
41. O'Brien, F. J.; Harley, B. A.; Yannas, I. V.; Gibson, L. J. *Biomaterials* **2005**, *26*, 433.
42. Engler, A. J.; Sen, S.; Sweeney, H. L.; Discher, D. E. *Cell* **2006**, *126*, 677.
43. Peyton, S. R.; Putnam, D. *J. Cell Physiol.* **2005**, *204*, 918.
44. Romberg, R. W.; Werness, P. G.; Riggs, B. L.; Mann, K. G. *Biochemistry* **1986**, *25*, 1176.
45. Gordeladze, J. O.; Reseland, J. E.; Duroux-Richard, I.; Apparailly, F.; Jorgensen, C. *ILAR J.* **2009**, *51*, 42.